Facies (2010) 56:385–397
DOI 10.1007/s10347-009-0210-8

ORIGINAL ARTICLE

Lacustrine microporous micrites of the Madrid Basin (Late Miocene, Spain) as analogues for shallow-marine carbonates of the Mishrif reservoir Formation (Cenomanian to Early Turonian, Middle East)

Chadia Volery · Eric Davaud · Anneleen Foubert · Bruno Caline

Received: 28 August 2009 / Accepted: 2 December 2009 / Published online: 22 December 2009

Abstract Shallow-marine microporous limestones account for many carbonate reservoirs. Their formation, however, remains poorly understood. Due to the lack of recent appropriate marine analogues, this study uses a lacustrine counterpart to examine the diagenetic processes controlling the development of intercrystalline microporosity. Late Miocene lacustrine microporous micrites of the Madrid Basin (Spain) have a similar matrix microfabric as Cenomanian to Early Turonian shallow-marine carbonates of the Mishrif reservoir Formation (Middle East). The primary mineralogy of the precursor mud partly explains this resemblance: low-Mg calcites were the main carbonate precipitates in the Cretaceous seawater and in Late Miocene freshwater lakes of the Madrid Basin. Based on hardness and petrophysical properties, two main facies were identified in the lacustrine limestones: a tight facies and a microporous facies. The tight facies evidences strong compaction, whereas the microporous facies does not. The petrotexture, the sedimentological content, and the mineralogical and chemical compositions are identical in both facies. The only difference lies in the presence of calcite overgrowths: they are pervasive in microporous limestones, but almost absent in tight carbonates. Early diagenetic transformations of the sediment inside a fluctuating meteoric phreatic lens are the best explanation for calcite overgrowths precipitation. Inside the lens, the dissolution of the smallest crystals in favor of overgrowths on the largest ones rigidifies the sediment and prevents compaction, while partly preserving the primary microporous network. Two factors appear essential in the genesis of microporous micrites: a precursor mud mostly composed of low-Mg calcite crystals and an early diagenesis rigidifying the microcrystalline framework prior to burial.

Keywords Microporosity · Micrite · Carbonate · Reservoir · Spain · Middle East

C. Volery (✉) · E. Davaud
Earth and Environmental Sciences, Department of Geology and Paleontology, University of Geneva, Rue des Maraîchers 13, 1205 Genève, Switzerland
e-mail: Chadia.Volery@unige.ch; chadia@infomaniak.ch

E. Davaud
e-mail: Eric.Davaud@unige.ch

A. Foubert
Department of Earth and Environmental Sciences, K.U. Leuven, Celestijnenlaan 200E, 3001 Heverlee, Belgium
e-mail: anneleen.foubert@ees.kuleuven.be

B. Caline
Total Exploration and Production, CSTJF, Avenue Laribau, 64000 Pau, France
e-mail: bruno.caline@total.com

Introduction

During the Cretaceous in the Middle East, the majority of stratigraphic stages contains one or more shallow-marine microporous carbonate reservoirs (Alsharhan and Nairn 2003; Volery et al. 2009). These reservoir formations are characterized by a microporous micritic matrix composed of sub-rhombic low-Mg calcite crystals with diameters generally below 8 μm. The mean porosity and permeability rate about 20% and few hundreds mD, respectively. Although several authors studied these particular limestones (Budd 1989; Lambert et al. 2006; Moshier 1989; Perkins 1989; Richard et al. 2007), some fundamental questions remain unresolved or are in controversy. Do the porosity and permeability develop during early or late diagenesis? Do the petrophysical qualities link to the

primary sedimentological or/and mineralogical content? What is the mineralogical composition of the precursor mud changing with diagenesis into a microporous limestone?

The last question was already debated in a previous paper (Volery et al. 2009): the study of stratigraphic occurrence of shallow-marine microporous carbonate formations in the Middle East reveals that such carbonates developed during periods of calcite seas. It clearly indicates that mud mainly composed of low-Mg calcite crystals is required to produce these microporous limestones. The relative stability of low-Mg calcite sediments in comparison to aragonite and high-Mg calcite muds partly explains the preservation of the primary microfabric and intercrystalline microporosity during diagenesis.

As recent shallow-marine muds are mostly aragonitic and high-Mg calcitic in composition, they cannot be used as a valuable analogue to study the formation of microporous limestones. However, freshwater lakes may represent interesting environmental counterparts, as low-Mg calcite often precipitates from lake water (Dean and Fouch 1983; Eugster and Kelts 1983; Kelts and Hsü 1978).

Late Miocene lacustrine microporous limestones of the Madrid Basin are characterized by similar mineralogy and microfabric as the Cenomanian to Early Turonian shallow-marine carbonates of the Mishrif reservoir Formation in the Middle East, but have a less complicated diagenetic history. In Iraq, for example, the Mishrif Formation underwent hydrocarbon loading and was buried under more than 3,700 m of Upper Cretaceous and Cenozoic sediments. On the contrary, the Late Miocene micrites of the Madrid Basin were covered with less than 100 m of Cenozoic sediments and have never experienced oil saturation. This study illustrates how lacustrine counterparts can be used to better understand diagenetic processes that control the formation and preservation of microporous micrites. In a similar way, Paleogene lacustrine chalky carbonates of the Madrid Basin were compared to marine pelagic chalks reservoirs (Arribas et al. 2004).

Geological setting

The Madrid Basin with an extension of more than 10,000 km^2 forms an important part of the Tajo Basin, one of the three large continental Cenozoic basins in the Iberian Peninsula. The Madrid Basin is a triangular intracratonic basin surrounded by three Cenozoic mountain ranges: the Spanish Central System in the northwest, the Toledo Mountains in the south, and the Iberian and Altomira ranges in the east (De Vicente et al. 1996a, 1996b). Alluvial, fluvial, and lacustrine sediments filled the Madrid Basin during the Cenozoic over a maximum thickness of 3,500 m (Junco and Calvo 1983).

Miocene deposits account for about one-third of the sedimentary record in the Madrid Basin. The sediments are subdivided into three units separated by discontinuities: the Lower, Intermediate, and Upper Units (Junco and Calvo 1983). As a consequence of Alpine movements, the Madrid Basin underwent compressive tectonics from the Late Oligocene. Stress fields changed into extensive regimes during the Late Miocene (Calvo et al. 1994; De Vicente et al. 1996a, 1996b).

The Upper Unit, which contains the formation described in this paper, is Turolian in age (Sanz et al. 1992) and is characterized by rivers and shallow freshwater carbonate lake deposits. While the lower part of the unit is mostly constituted by fluvial and alluvial sediments, lacustrine beds become mainly dominant in the upper part (Calvo et al. 1996). Warm and dry climate conditions prevailed during the deposition of the Upper Unit (Calvo et al. 1993; Sanz et al. 1992).

Late Miocene lacustrine limestones of the Madrid Basin were chosen because low-Mg calcite was often the primary precipitate in these freshwater lakes (Bellanca et al. 1989; Calvo et al. 1995; Utrilla et al. 1998). Lacustrine carbonates were sampled in the quarry of Colmenar de Oreja (Fig. 1) where they are surrounded by palustrine facies (Wright et al. 1997). The top of the sedimentary record in the quarry is affected by karstification and no Pliocene

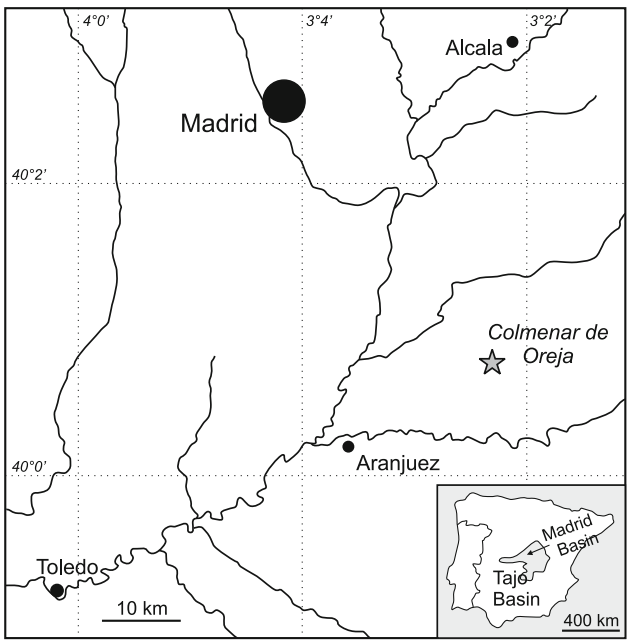

Fig. 1 The Colmenar de Oreja quarry (40°07′44″N and 03°23′04″W) is situated in Central Spain in the Madrid Basin, which forms an important part of the Tajo Basin

sediments exist (Instituto geologico y minero de Espana 1975).

Methods

The studied profile measures 162 cm. Sampling was done with a vertical resolution of about 10 cm. In the cohesive layers, 13 samples were taken (samples 1–12 and 9top). Duplicates were sampled in the same level at about 1 m laterally from the reference log. In total, 26 thin-sections were prepared for petrographical analyses. In the poor cohesive layers, five samples were taken (samples S1–S5), but they were too friable to allow the preparation of representative thin-sections.

Thin-sections were studied with classical petrographical techniques using light microscopy and cathodoluminescence. The content in charophytes (associated with few ostracods) and the percentage of matrix were quantified. Calcite overgrowths intensity was evaluated. Cathodoluminescence studies did not reveal any significant luminescence.

Scanning electron microscopy (SEM) was performed on 18 fragments from each of the different sampled layers (samples 1–12, 9top, and S1–S5). Microfabrics were studied on samples coated with gold. The SEM analyses were carried out in Total laboratories (Pau, France) with a Leo 1450VP. The working current was set at 15 kV.

Porosity (phi), permeability (K), and capillary pressure (Cp) were measured in Total laboratories. In order to prevent isolated non-representative heterogeneity (large bioclasts, vugs, cracks caused by the plugging), two plugs were drilled from each of the 26 cohesive samples. Some layers were too friable to take representative plugs. In total, porosity and permeability were analyzed on 35 plugs. The porosity was measured with helium. The permeability was calculated with nitrogen and corrected for the Klinkenberg effect. The capillary pressure was performed for eight specific samples (samples 1, 2, 4, 5, 9, 10, 11, and 12) with the Purcell method in an Autopore IV of Micrometrics.

The mineralogical and chemical composition of 20 samples coming from the 18 identified layers was identified by X-ray diffraction (XRD) and X-ray fluorescence (XRF) analyses. Diffraction peaks were measured for angles from 4.5° to 70°. The XRD device was an XPert Pro of Panalytical and the XRF device a Pioneer S4 of Bruker.

The stable isotopic composition of O and C was measured on seven whole-rock samples (samples S2, 3, 5, 6, 8, 10, and 12) with the AP2003 mass spectrometer of Analytical Precision. Values were normalized with the reference material NBS 19 (TS-Limestone).

Results

Lacustrine limestones in the quarry of Colmenar de Oreja are characterized by centimeter-sized beds presenting variable degrees of cohesion (Fig. 2). Very friable layers alternate with semi-cohesive chalky beds, cohesive chalky ones, and hard limestones. The lacustrine section presented in this study is situated on top of palustrine facies. The section starts with chalky layers and ends with 20 cm of hard limestones. On top of the described profile, more lacustrine chalky layers are present. There is no remarkable surface in the studied section.

Petrography and petrophysical properties

Petrographical observations and petrophysical measurements show that the lacustrine micrites of Colmenar de Oreja are divisible into two main facies: a tight facies and a microporous one. On the macroscopic scale, the tight facies corresponds to hard layers and the microporous facies to chalky beds.

Tight facies (T)

Carbonates of the tight facies (T) are hard as typical lithographic limestones. Samples are wackestones rich in charophytes with some ostracods (Fig. 3a–b). The concentration in charophytes rates about 20%. Tests are strongly squashed; they underwent compaction (Fig. 3a–b, *arrows*). Only a few calcite overgrowths exist around some charophytes. The muddy matrix is dark. Under the SEM, the matrix of the tight facies presents a serrate to meshed microfabric (Loreau 1972) (Fig. 3c–d). Crystals have rhombic shapes with sizes generally smaller than 4 μm. Clusters of crystals with no well-defined faces are larger than 4 μm (Fig. 3d, *arrows*). SEM pictures show that almost no intercrystalline microporosity exists. Porosities and permeabilities of the T facies, respectively, range from 8 to 18% and from 0.02 to 5.62 mD (Figs. 4, 5; Table 1). Pore threshold radii rate between 0.1 and 0.4 μm (Fig. 5; Table 1). Plugs coming from the same layer present close values. A gradual diminution of the petrophysical qualities occurs from the sample 10 to the sample 12.

Microporous facies (M3, M2, M1)

Layers from the microporous facies are very chalky. They are composed of wackestones rich in charophytes with a few ostracods (Fig. 3e–f). The percentage of bioclasts rates about 20 to 30%. Tests are morphologically preserved; they are neither broken nor squashed. Matrix and charophyte

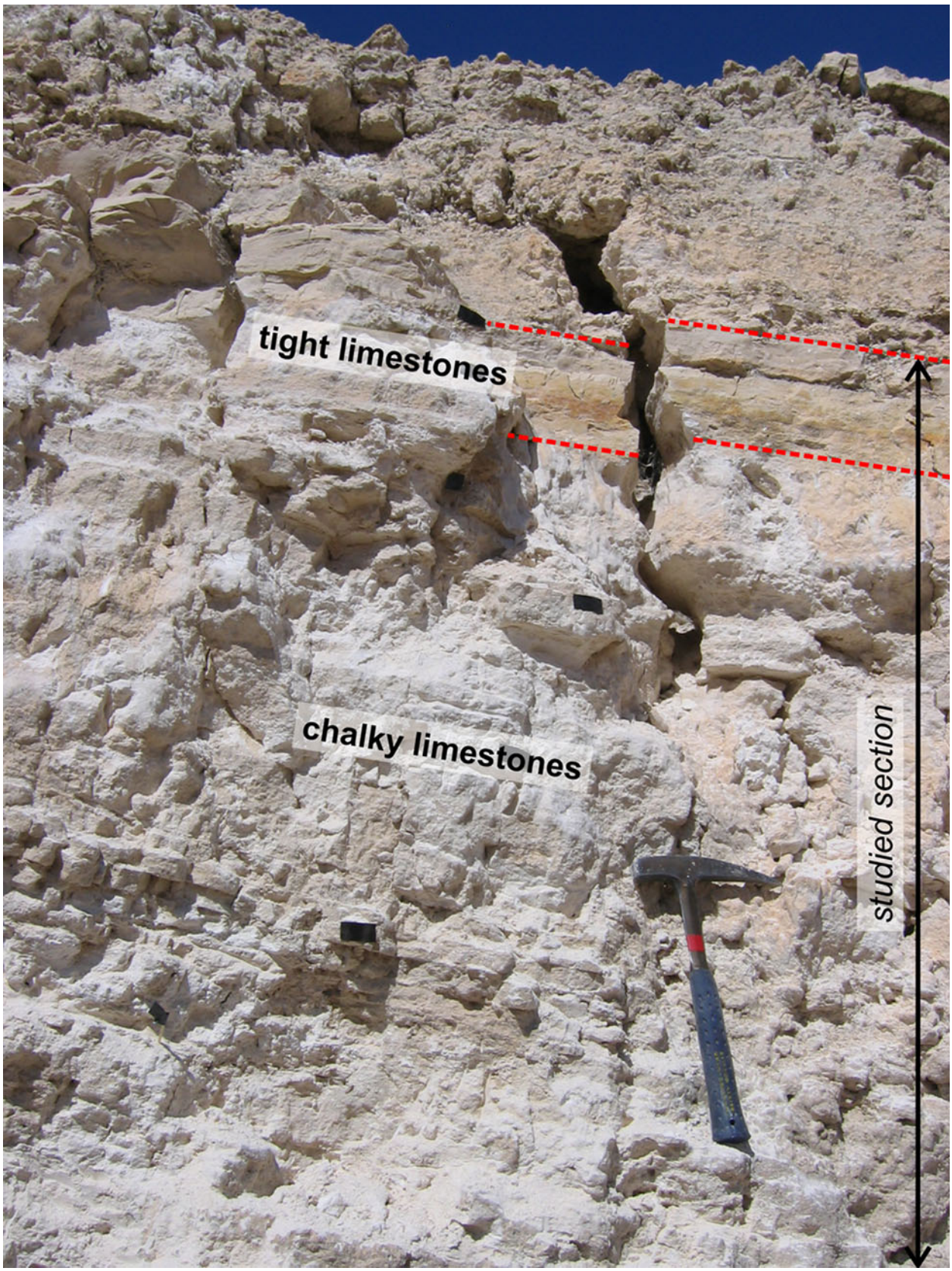

Fig. 2 The studied section is composed of chalky limestones (alternations of friable, semi-cohesive, and cohesive chalky beds) topped by tight limestones. Chalky limestones repeat after the tight limestones

crystals underwent calcite overgrowths. The muddy matrix is clearer than in the T facies.

Based on cohesion and hardness, calcite overgrowths, and petrophysical properties, the microporous facies can be subdivided into three sub-facies: a cohesive (M3), a semi-cohesive (M2), and a friable one (M1).

Carbonates of the cohesive microporous facies (M3) occur as relatively solid but still chalky layers. Calcite overgrowths are pervasive. Under the SEM, the matrix shows a punctic to serrate microfabric (Loreau 1972) (Fig. 3g–h). The largest crystals reach about 10 μm in size and present rhombic shapes (Fig. 3h, *arrows*). They are often linked to charophytes test. The smallest crystals (~2 μm) have rounder shapes. Intercrystalline microporosity is considerably present. The M3 samples have high porosities and permeabilities spreading from 23 to 36% and from 23 to 1,516 mD, respectively (Figs. 4, 5; Table 1). Pore threshold radii value about 8 to 11 μm (Fig. 5; Table 1). Samples from a same layer often possess values close together.

Limestones of the semi-cohesive microporous facies (M2) are softer and more friable than the ones from the M3 facies. Calcite overgrowths are present but generally less developed. SEM observations allowed to identify a punctic microfabric (Loreau 1972) of the matrix. The largest crystals are about 6 μm in size and they are sub-rhombic in shape with blunted edges. The smallest crystals reach about 2 μm and they are rounded. The microcrystalline framework has a high intercrystalline microporosity. Limestones from the M2 facies have very high values of porosities and permeabilities (Figs. 4, 5; Table 1). The first feature varies between 35 and 46% and the second between 187 and 2,780 mD. Pore threshold radii rate about 8 to 11 μm (Fig. 5; Table 1). Homogeneous values generally exist throughout the same layer.

The friable microporous facies (M1) is so chalky that the sampling of consolidated fragments was impossible. Nevertheless, with the SEM, charophytes and microcrystalline calcites could be observed. Crystal sizes reach up to 6 μm. All crystals present very round shapes.

Mineralogical composition

The analyses with XRD and XRF show an extremely monotonous mineralogical composition throughout all the samples: 98–99% of calcite and the rest of quartz (Table 2). No variation exists between the tight and the microporous facies or inside the three different microporous facies. Clay is totally absent in any sample. The magnesium and the strontium contents vary between 0.12 and 0.31% and between 156 and 380 ppm, respectively. No relation can be observed between the magnesium or the strontium evolution and the tight or the microporous facies occurrence.

Stable isotopes

The stable isotopic composition is very constant for all the samples (Fig. 5; Table 2). The $\delta^{18}O$ ratio varies between −6.5 and −5.7‰ PDB and the $\delta^{13}C$ between −10.3 and −9.1‰ PDB. Oxygen values are comparable to those found in freshwater lakes of the Madrid Basin at the end of the Middle Miocene, but carbon values are a bit more negative (about 2.0‰ less) (Bellanca et al. 1992). There is no constant difference in the $\delta^{18}O$ or the $\delta^{13}C$ ratio depending on the facies.

Discussion

Similarities between lacustrine and marine micrites

First of all, the obvious resemblance in microfabric between lacustrine microporous micrites of Colmenar de Oreja (Spain, Late Miocene) and shallow-marine microporous micrites of the Mishrif reservoir Formation (Middle-East, Cenomanian to Early Turonian) must be highlighted (Fig. 6). SEM observations reveal that the matrix of both carbonates presents a microporous network constituted by low-Mg calcite crystals rhombic to sub-rhombic in shape and with mean diameters generally below 8 μm. Moreover, both limestones also possess tight layers composed of meshed to coalescent microfabric (Loreau 1972) with anhedral crystals.

However, the sedimentological facies are very different between the marine micrites of the Mishrif Formation (Middle East, Cenomanian to Early Turonian) and the lacustrine micrites of the Madrid Basin (Spain, Late Miocene). The Mishrif Formation is made of bioclastic and peloidal limestones (mainly mudstones to packstones and floatstones) rich in rudists, bivalves, echinoderms, foraminifera, and algae, while the studied lacustrine micrites from the Madrid Basin are only constituted of wackestones with charophytes.

This similarity of microfabrics confirms the essential role played by the mineralogical composition of the precursor mud in the development of such microporous limestones (Volery et al. 2009). During the Cenomanian to Early Turonian, the seawater was favorable to the precipitation of low-Mg calcite (Dickson 2002, 2004; Hardie 1996; Lowenstein et al. 2001; Sandberg 1983; Siemann 2003). Moreover, rudists, organisms mainly composed with low-Mg calcite, were principal carbonate builders (Stanley and Hardie 1998). During the Late Miocene in Spain, freshwater lakes were characterized by low-Mg calcite precipitation

(Bellanca et al. 1989; Calvo et al. 1995; Utrilla et al. 1998) and charophytes proliferation, organisms with pure low-Mg test. Thus, in both cases, the precursor mud was mainly composed of low-Mg calcite crystals.

Such mineralogical prerequisite is easily explained in terms of stability. Aragonite, and to a lesser extent high-Mg calcite, have to transform into their polymorph of low-Mg calcite to acquire relative chemical stability. In consequence, they completely lose their primary microfabric. Limestones issued from this transformation present bad intercrystalline microporosity (Lasemi and Sandberg 1984). On the contrary, original low-Mg calcite crystals are already in a stable form. Their primary microfabric and microporous network can partly be preserved during diagenesis.

Similarly, the low-Mg calcite nature of coccolith test fragments composing chalk reservoirs (as widespread in the North Sea) partly explains the preservation of the intercrystalline microporosity in these sediments.

Differences between the microporous and the tight facies

Very contrasting petrophysical properties characterizes, respectively, the tight and microporous micrites of Colmenar de Oreja. Tight layers always have values of porosity below 20% and permeability lower than 10 mD, while the microporous facies generally has porosities ranging from 25 to 45% and permeabilities from several 100 mD up to about 2,500 mD. Pore threshold radii vary from less than 1 μm for the tight facies to about 10 μm for the microporous one. Macroporosity due to charophyte stems forms an important part of the total porosity. As the content of charophytes remains constant throughout the profile, the intercrystalline microporosity has not been estimated and considered as proportional to the total porosity.

Beds of the tight facies are hard limestones, whereas layers of the microporous one are chalky carbonates. The tight facies evidences strong compaction features such as squashed charophytes, while the microporous facies exhibit morphologically intact charophytes tests and do not present any other signs of compaction.

This differential compaction is surprising as the petrographical texture and the sedimentological content of both facies are identical. Mineralogical and chemical analyses show no significant differences in composition. Clays are totally absent; thus they could not be involved as a factor of compaction (Ehrenberg 2004; Ehrenberg and Boassen 1993; Lambert et al. 2006). The strontium content does not indicate aragonite enrichment (Lasemi and Sandberg 1993) in tight layers that may speak in favor of a differential diagenesis as in limestone-marl alternations (Munnecke and Samtleben 1996; Westphal 2006). The stable isotopes present too little variations ($\Delta\delta^{18}O = 0.8‰$ and $\Delta\delta^{13}C = 1.2‰$) to be significant (Bellanca et al. 1992; Eugster and Kelts 1983; Leng et al. 2006; Lerman 1978). To conclude, neither the sedimentological content nor the chemical and mineralogical composition can be the cause of the differential compaction.

Fig. 3 **a**, **b** Tight facies: wackestones composed of squashed charophytes (*arrows*) inside a dark micritic matrix. **c**, **d** Tight facies (SEM pictures): serrate to meshed microfabric made of subhedral rhombic crystals with size generally below 4 μm and clusters of crystals with no well-defined faces (**d**, *arrows*). **e**, **f** Microporous facies: wackestones composed of unbroken charophytes with calcite overgrowths inside a light matrix showing intensive calcite overgrowths. Abundant macroporosity and microporosity. **g**, **h** Microporous facies (SEM pictures): punctic to serrate microfabric made of euhedral rhombic crystals up to 10 μm in size (**h**, *arrows*) and rounder smaller ones ▶

However, in microporous micrites preserved from compaction, calcite overgrowths are ubiquitous, while this feature is almost totally absent in limestones of the tight facies. This clearly suggests that calcite overgrowths occurred during early diagenesis and prevented compaction.

When a dissolution-reprecipitation occurs throughout carbonates of homogenous mineralogical composition, the smallest crystals are the most unstable and are dissolved in favor of overgrowths of largest crystals, the ones with the lowest energy state. This process is called Ostwald ripening (Baronnet 1982; Morse and Casey 1988; Ostwald 1887). In low-Mg calcite micrites of Colmenar de Oreja, observations with the SEM support this process. The microporous limestones are made up of a punctic to serrate framework (Loreau 1972) with rhombic large calcites (<10 μm) and small rounder ones (~2 μm) (Fig. 7). So, the most euhedral crystals are the largest, and the smallest ones evidences dissolution. Ions of small calcites probably nourished overgrowths of large ones.

On the contrary, samples of tight facies generally present a serrate to meshed microfabric (Loreau 1972) built by small rhombic crystals, less than 4 μm in size, and larger clusters with no well-defined faces (<10 μm). Euhedral crystals never reach the size of 6 to 10 μm as they do in the microporous facies. Clusters are probably the result of compaction of several small crystals. The lack of large euhedral crystals indicates that calcite overgrowths never occurred inside the tight facies with the same intensity as in the microporous one.

Micritic muds that have benefited from calcite overgrowths were preserved from compaction. This partial early cementation controlled by the Ostwald ripening process (Baronnet 1982; Morse and Casey 1988; Ostwald 1887) permits to rigidify the carbonate sediment while globally preserving the original fabric and primary

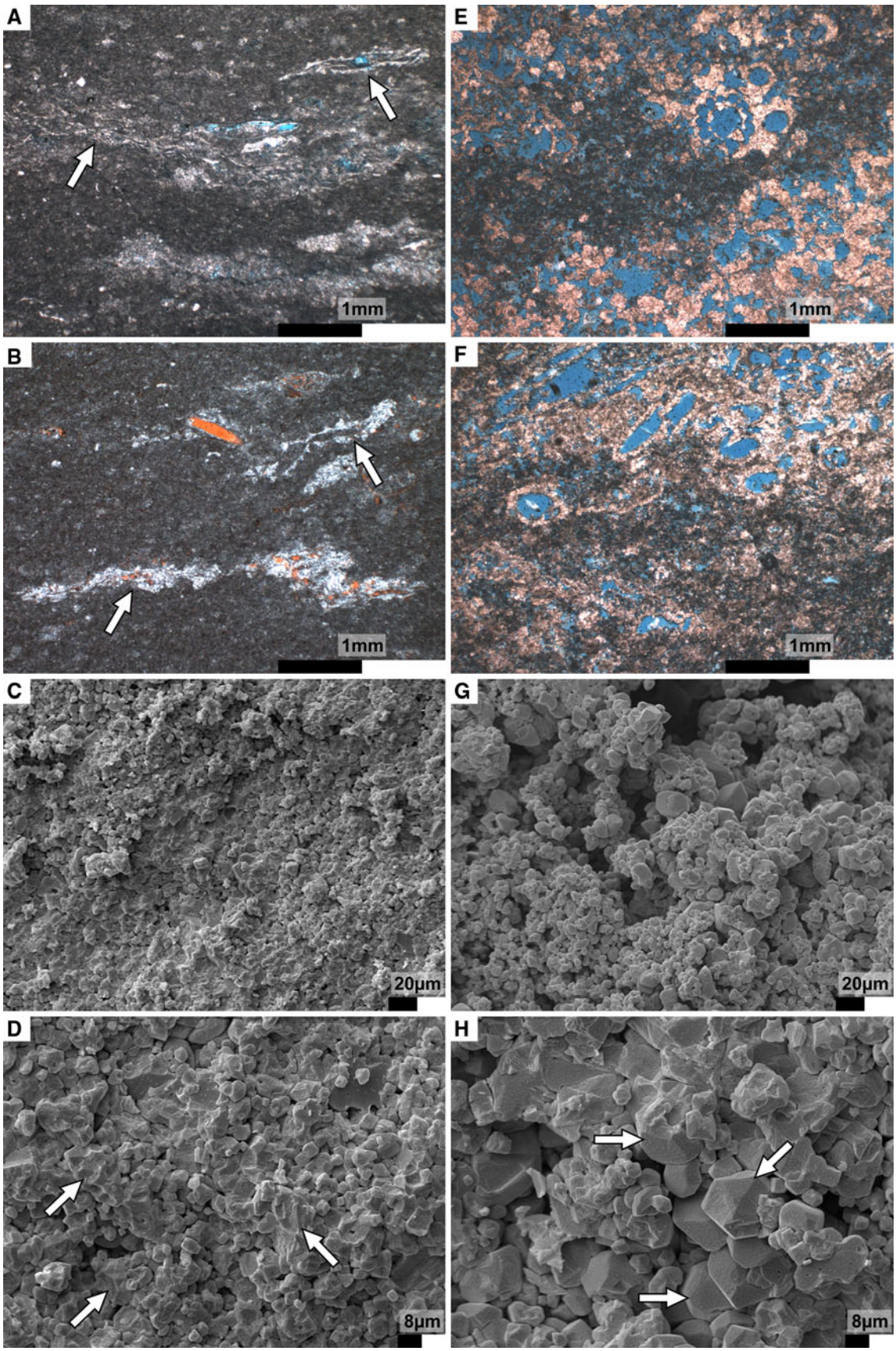
A
1mm
E
1mm
B
1mm
F
1mm
C
20μm
G
20μm
D
8μm
H
8μm

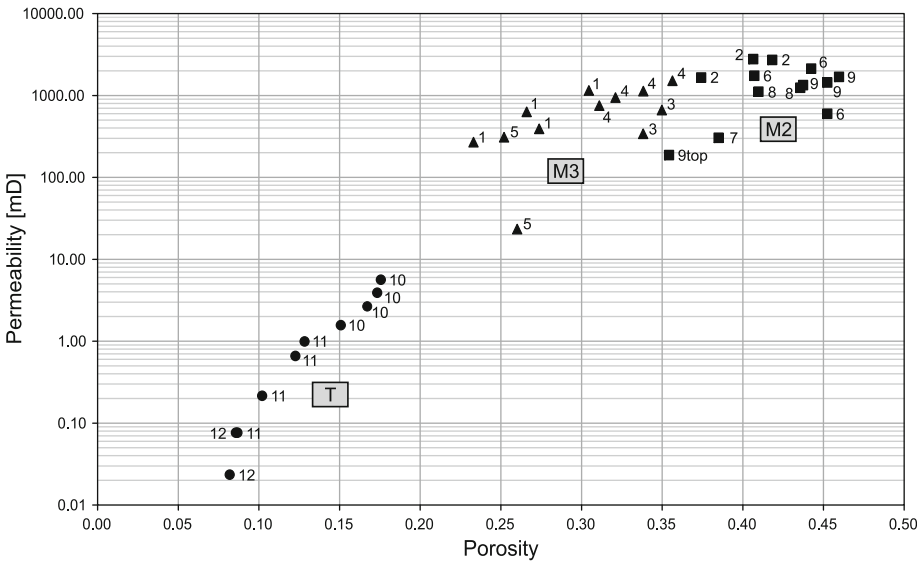

Fig. 4 Porosities and permeabilities of samples from the tight facies (*T*, *circles*), the semi-cohesive microporous facies (*M2*, *squares*) and the cohesive microporous one (*M3*, *triangles*). Samples of the friable microporous facies (*M1*) were not measured because of the impossibility of taking plugs in these very chalky layers. Same number corresponds to different sample but same layer

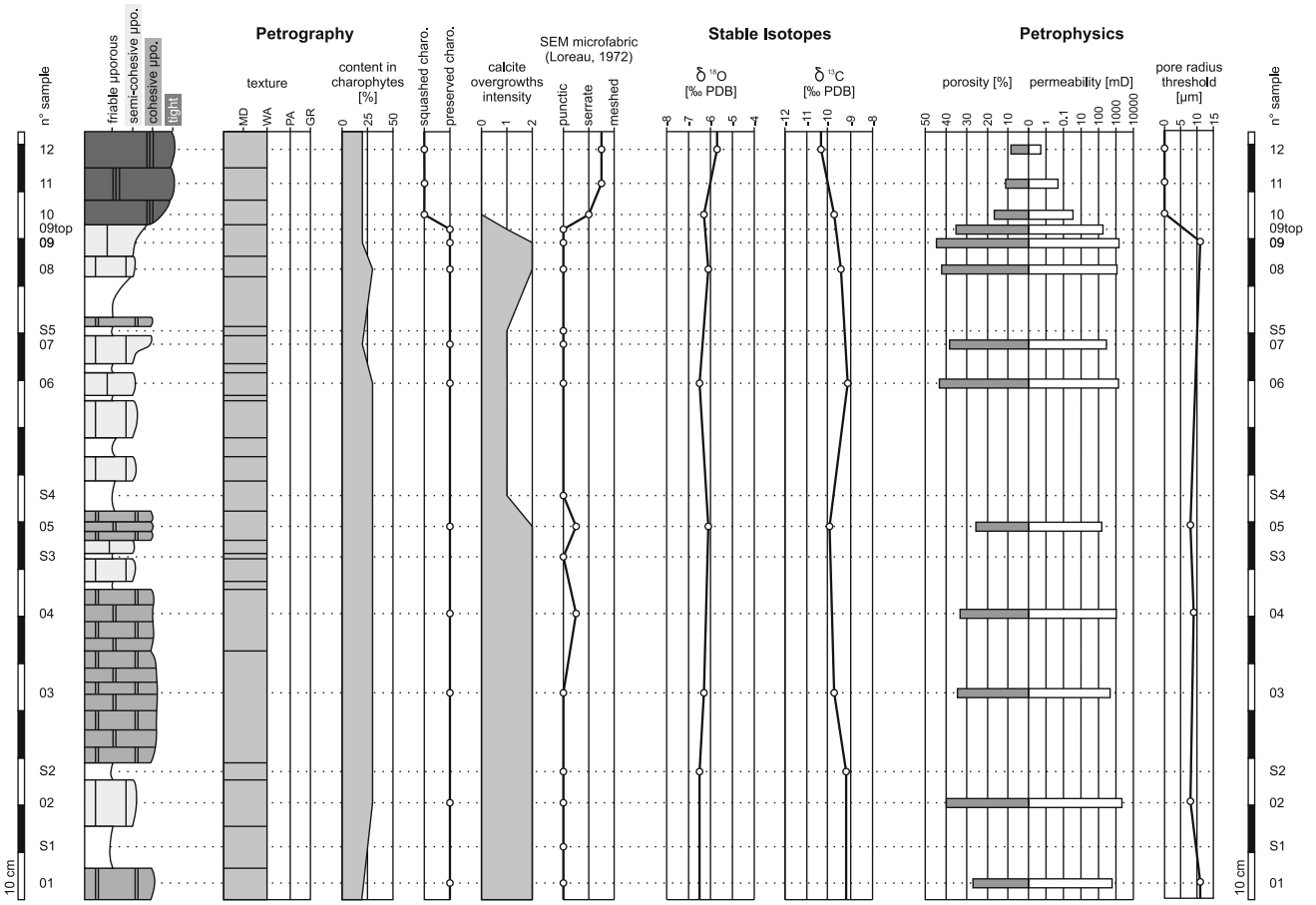

Fig. 5 Synthetic log with petrographical descriptions, stable isotopes values, and petrophysical properties. The texture, the sedimentological content, and stable isotopes values are very constant throughout the section. The compaction is correlated to the absence of calcite overgrowths. Samples that have undergone compaction (10, 11, and 12) possess serrate to meshed microfabrics and bad petrophysical properties

Table 1 Values of porosity (phi), permeability (K), and pore threshold radius from capillary pressure (Cp) for samples 1 to 12 and 9top

		phi	*K* (mD)	Cp (μm)
1	a	0.23	269	
	b	0.30	1,152	
	c	0.27	392	10.83
	d	0.27	631	
	Mean	0.27	611	
2	a	0.41	2,780	
	b	0.42	2,715	
	c	0.37	1,650	7.97
	Mean	0.40	2,382	
3	a	0.34	341	
	b	0.35	663	
	Mean	0.34	502	
4	a	0.34	1,131	
	b	0.36	1,516	
	c	0.31	752	9.29
	d	0.32	946	
	Mean	0.33	1,086	
5	a	0.25	310	7.97
	b	0.26	23	
	Mean	0.26	167	
6	a	0.41	1,739	
	b	0.44	2,118	
	c	0.45	596	
	Mean	0.43	1,484	
7	a	0.38	304	
8	a	0.44	1,239	
	b	0.41	1,108	
	Mean	0.42	1,173	
9	a	0.44	1,338	
	b	0.46	1,681	
	c	0.45	1,437	10.83
	Mean	0.45	1,485	
9	Top	0.35	187	
10	a	0.17	2.65	0.43
	b	0.17	3.90	
	c	0.18	5.62	
	d	0.15	1.57	
	Mean	0.17	3.44	
11	a	0.13	0.99	
	b	0.12	0.66	
	c	0.09	0.08	0.13
	d	0.10	0.22	
	Mean	0.11	0.49	
12	a	0.09	0.08	0.23
	b	0.08	0.02	
	Mean	0.08	0.05	

High porosity, permeability, and pore threshold radius values characterize samples 1 to 9 of the microporous facies

Low porosity, permeability, and pore threshold radius values characterize samples 10 to 12 of the tight facies

intercrystalline microporosity. With a limited external source of calcium carbonate, the sediment only undergoes a reshaping of its microfabric. In theory, no porosity should be lost by this way. On the contrary, the microporous network may even acquire better petrophysical properties as the Ostwald ripening process makes it more homogenous by eliminating small crystals and forming a larger and more uniform grain size.

Late Miocene lacustrine deposits underwent only a shallow burial (maximum 80 m) (Calvo et al. 1994). However this was sufficient to drastically reduce the porosity (about 20% loss) and the permeability (more than 2,000 mD loss) of non early cemented muds.

Diagenetic models

Based on previous observations, two early diagenetic scenarios can be considered. Late diagenesis was dominated by the Pliocene exposure of the Madrid Basin (Sanz 1994).

Early diagenesis: scenario 1

The reason of the differential compaction may stem from paleoenvironmental changes during the low-Mg calcite production. Because of physicochemical modifications in the lake (e.g., pH, alkalinity, temperature, water stratification, or complete circulation, primary productivity…), the size of precipitated crystals may change through time (Teranes et al. 1999). In layers composed of large crystals, fluids circulate and calcite overgrowths are intensive. On the contrary, in layers made of smaller crystals, the bad permeability prevents calcite overgrowths. These uncemented sediments will be strongly compacted under lithostatic pressure (tight facies), while early cemented layers will resist compaction and partly preserve their primary microfabric with intercrystalline microporosity (microporous facies).

Early diagenesis: scenario 2

Compaction differences may originate from early diagenetic processes without influences from the primary lithology. The low-Mg calcite accumulation occurs homogenously in a shallow freshwater lake (Bellanca et al. 1989; Calvo et al. 1995; Utrilla et al. 1998). When the lacustrine sedimentation ends due to hydrological changes, a meteoric phreatic lens may develop, fluctuating throughout the lacustrine deposits. Ions exchanges occur inside the phreatic lens, mostly at its top as the contact with CO_2-rich air and the evaporative pumping increase the ionic strength just below the water surface. There, the smallest crystals are slightly dissolved and nourish overgrowths on the largest ones. Moreover, when dissolution

Table 2 Bulk compositions, CaO, MgO, and SrO contents, stable isotopic ratios of samples S1 to S5, 1 to 12 and 9top

	Calcite (% mass)	Quartz (% mass)	CaO (% mass)	MgO (% mass)	SrO (ppm)	$\delta^{13}C$ (‰PDB)	$\delta^{18}O$ (‰PDB)
S1	99.70	0.27	55.16	0.22	356		
S2	99.30	0.68	55.14	0.24	376	−9.2	−6.5
S3	98.10	1.90	53.82	0.26	298		
S4	99.20	0.79	54.97	0.24	318		
S5	99.60	0.38	55.76	0.19	306		
1	99.80	0.20	55.22	0.29	380		
2	99.80	0.16	56.20	0.16	228		
3	99.90	0.14	55.56	0.19	224	−9.7	−6.3
4	99.80	0.15	56.61	0.13	156		
5	99.20	0.77	55.77	0.19	205	−9.9	−6.1
6	99.50	0.45	55.84	0.15	272	−9.1	−6.5
7	99.70	0.34	55.62	0.27	274		
8	99.80	0.20	56.22	0.15	239	−9.4	−6.1
9	99.70	0.30	55.68	0.27	284		
9 top	99.60	0.43	55.72	0.18	257		
10	99.60	0.41	56.02	0.12	246	−9.7	−6.3
11	99.60	0.38	56.00	0.13	260		
12	99.60	0.38	55.63	0.31	278	−10.3	−5.7

Lacustrine limestones of Colmenar de Oreja are almost only composed of low-Mg calcite. Stable isotopic values are very constant throughout the profile (rem: value 12 was measured during a different series)

occurs under occasional rain in the vadose zone, ions go down by percolation and enrich the top of the phreatic lens. Overgrowths are in this case dominant. All these processes permit carbonate muds to rigidify.

Depending on climatic conditions, the water table may have varied vertically (Fig. 8). Thus lacustrine horizons affected by this dissolution-reprecipitation and its associated partial early cementation change during times. Numerous different layers may be affected by theses processes. In this case, the bedding observed at the outcrop is purely diagenetic.

However, some muds always remain situated outside the physicochemical active zone of the phreatic lens and are not affected by this dissolution-reprecipitation process. They will suffer strong compaction during burial, contrary to early cemented muds.

The presence of palustrine facies a few meters above these lacustrine limestones (Wright et al. 1997) supports

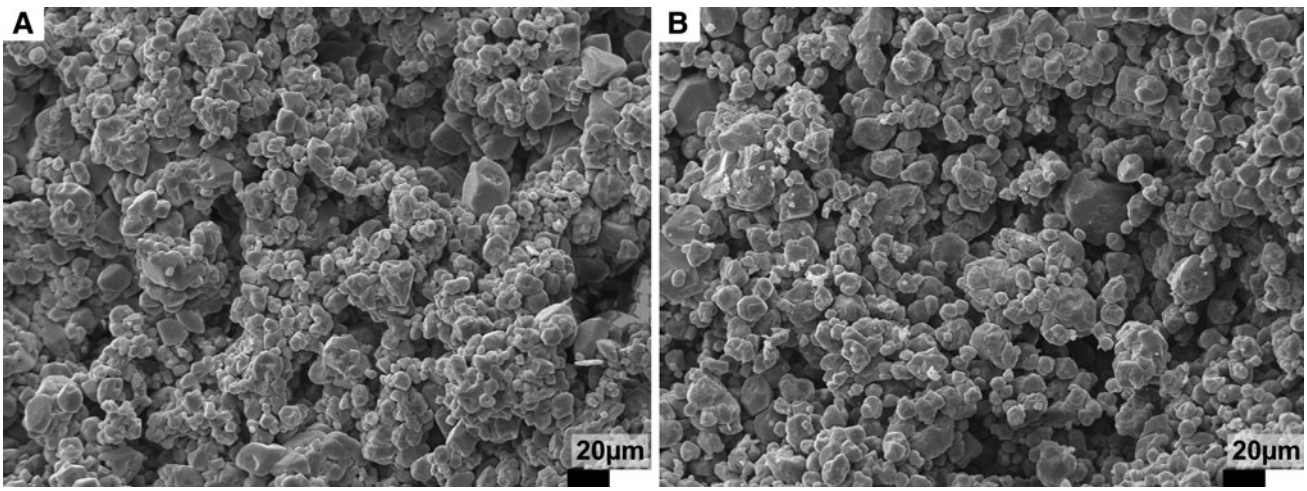

Fig. 6 The obvious resemblance in microfabrics between **a** Late Miocene lacustrine microporous micrites of Colmenar de Oreja (Spain) and **b** Cenomanian to Early Turonian shallow-marine microporous carbonates of the Mishrif reservoir Formation (Qatar)

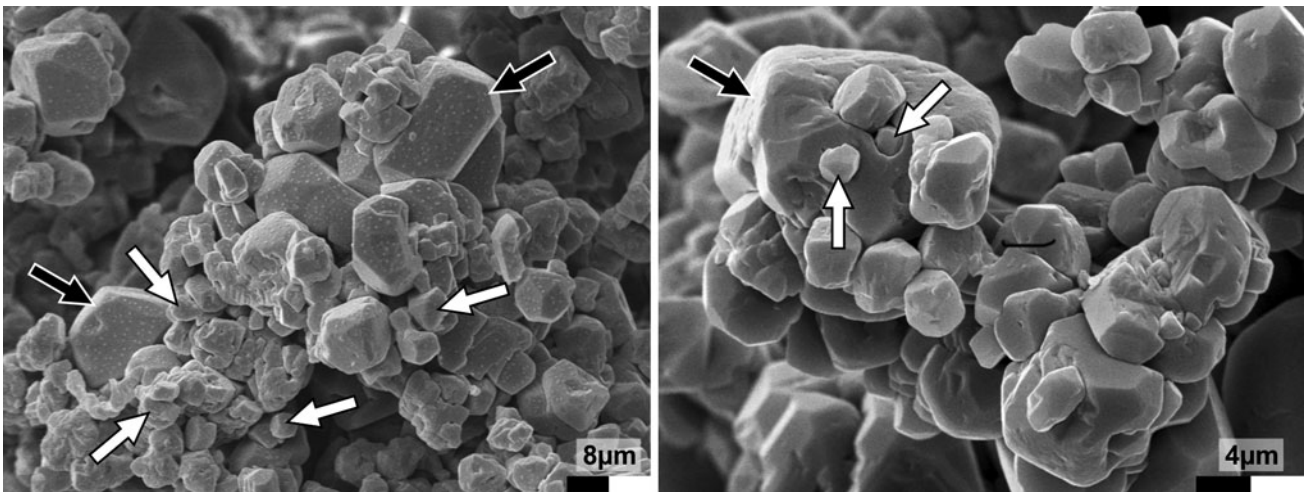

Fig. 7 SEM pictures from the microporous facies of the lacustrine micrites of Colmenar de Oreja (Late Miocene, Spain) showing a bi-modal grain size (*left picture*: sample 04, *right picture*: sample 03). The smallest crystals were preferentially dissolved (*rounded shapes*, *white arrows*) and nourished overgrowths of largest ones (*euhedral rhombic shapes*, *black arrows*). This particular bi-modal grain-size supports a dissolution-reprecipitation by Ostwald ripening process. In the right picture, small crystals (*white arrows*) are merged into a larger crystal (*black arrow*)

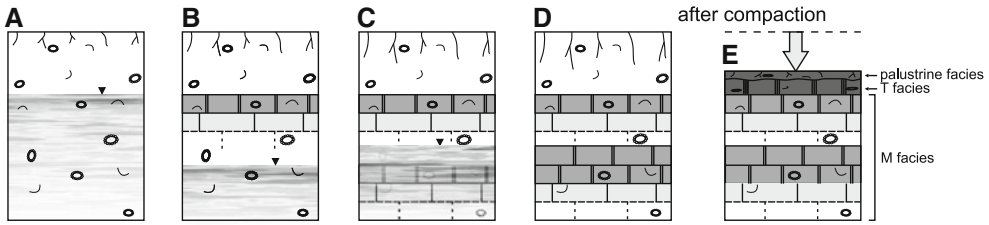

Fig. 8 Sketch illustrating the early diagenetic model of the scenario 2. **a** After the lacustrine sedimentation, a phreatic lens develops. In the ionic active zone situated at the top of the lens, lacustrine muds undergo dissolution-reprecipitation by Ostwald ripening and rigidify themselves. The ionic strength diminishes with distance to the water table top. Beds situated close to the water table surface are further rigidified than the ones located deeper (*grey levels*). **b**, **c** The phreatic lens fluctuates and new horizons are rigidified by the Ostwald ripening process. **d** Hypothetical situation before compaction. **e** With burial, early cemented layers resist compaction and partly preserve their primary microfabric and intercrystalline microporosity (*M facies*), while uncemented ones are strongly compacted and become tight limestones (*T facies*). (Meaning of *grey levels* corresponds to ones of Fig. 5)

the existence of a phreatic lens after the lacustrine sedimentation. Moreover, with this diagenetic scenario, the different hardness of the three microporous sub-facies may be explained in terms of residence time inside the ionic active water. Indeed, cohesive microporous limestones (M3) probably stayed longer inside the active zone of the phreatic lens than semi-cohesive ones (M2), or still more than friable ones (M1). In the M3 facies, dissolution and reprecipitation processes had more time to cement the carbonate sediment and led to the present most cohesive beds. On the contrary, M1 muds benefited during only a relative short time of this early cementation and are actually the least resistant layers. M2 limestones result from an intermediate state. In fact, microporous samples of Colmenar de Oreja could be described inside a continuous diagram of petrographical and petrophysical properties. These observations and data confirm the transformation of their microfabric with a gradual diagenesis.

Late diagenesis

After the early compaction, lacustrine microporous and tight facies were probably submitted to similar diagenetic conditions. Carbonate deposits were exposed during the Pliocene, leading to intensive karst development (Sanz 1994). Because of their high permeability, friable microporous layers (M1) underwent strong dissolution, as demonstrated by the abundance of small round crystals in the matrix. This could explain the very poor cohesion of M1 limestones. The dissolution necessarily

comes after the compaction, because such friable rocks cannot have resisted the lithostatic pressure. The M2 and M3 facies were also affected by late dissolution, but less intense. The relative pronounced early cementation in M2 and M3 layers partly protected them from further dissolution.

Lacustrine carbonates of the tight facies show no dissolution signs. After compaction, the microfabric was quasi impermeable to fluids and thus protected from dissolution.

Conclusions

The remarkable similarity in the microfabrics of the Cenomanian to Early Turonian shallow-marine microporous carbonates from the Mishrif reservoir Formation in the Middle East and the Late Miocene lacustrine microporous micrites from the Madrid Basin in Spain is not a coincidence. In both environments, the precursor sediment was mainly composed of low-Mg calcite crystals. The relative stability of such carbonate mud permits the partial preservation of the original microfabric and the primary intercrystalline microporosity under moderate diagenesis.

Lacustrine limestones of Colmenar de Oreja are made of a microporous and a tight facies with contrasting petrophysical properties. These differences cannot be linked to the texture and sedimentological content or to the mineralogical and chemical composition. Tight limestones evidenced strong compaction, while microporous carbonates remained non-compacted. Intensive calcite overgrowths on matrix and charophytes crystals are present in the microporous facies. Obviously, they have created a rigid framework that prevented compaction.

Circumstances in which calcite overgrowths occurred are badly constrained with the available data. The differential lithification probably results from early diagenetic transformations (dissolution-reprecipitation by Ostwald ripening process) linked to a fluctuating meteoric phreatic lens. This hypothesis is supported by the presence of palustrine deposits over the lacustrine sequence.

The study of lacustrine micrites of Colmenar de Oreja (Spain, Late Miocene) shows that two factors seem essential for forming microporous limestones: (1) a precursor mud mostly composed of low-Mg calcite crystals, and (2) an early diagenesis rigidifying the microcrystalline framework prior to shallow burial.

Acknowledgments This research was funded by the University of Geneva and by Total Exploration and Production. The review of a previous version of the manuscript by Axel Munnecke (University of Erlangen) is acknowledged with thanks.

References

Alsharhan AS, Nairn AEM (2003) Sedimentary basins and petroleum geology of the Middle East. Elsevier, Amsterdam, p 843

Arribas ME, Bustillo A, Tsige M (2004) Lacustrine chalky carbonates: origin, physical properties and diagenesis (Palaeogene of the Madrid Basin, Spain). Sediment Geol 166(3–4):335–351

Baronnet A (1982) Ostwald ripening in solution–the case of calcite and mica. Estud Geol 38:185–198

Bellanca A, Calvo JP, Censi P, Elizaga E, Neri R (1989) Evolution of lacustrine diatomite carbonate cycles of Miocene age, southeastern Spain; petrology and isotope geochemistry. J Sediment Res 59(1):45–52

Bellanca A, Calvo JP, Censi P, Neri R, Pozo M (1992) Recognition of lake-level changes in Miocene lacustrine units, Madrid Basin, Spain. Evidence from facies analysis, isotope geochemistry and clay mineralogy. Sediment Geol 76(3-4):135–153

Budd DA (1989) Micro-rhombic calcite and microporosity in limestones: a geochemical study of the Lower Cretaceous Thamama Group, U.A.E. Sediment Geol 63(3–4):293–311

Calvo JP, Daams R, Morales J, Lopez-Martinez N, Agusti J, Anadon P, Armenteros I, Cabrera L, Civis J, Corrochano A, Diaz-Molina M, Elizaga E, Hoyos M, Martin-Suarez E, Martinez J, Moissinet E, Muñoz A, Perez-Garcia A, Perez-González A, Porttero JM, Robles F, Santisteban C, Torres T, Van Der Meulen AJ, Vera JA, Mein P (1993) Up-to-date Spanish continental Neogene synthesis and paleoclimatic interpretation. Rev Soc Geol Esp 6(3–4):29–40

Calvo JP, Ordonez S, Garcia del Cura MA, Hoyos M, Alonso Zarza AM (1994) Madrid Basin (Neogene), Spain. In: Gierlowski-Kordesch E, Kelts K (eds) Global geological record of lake basins. University Press, Cambridge, pp 303–305

Calvo JP, Jones BF, Bustillo M, Fort R, Alonso Zarza AM, Kendall C (1995) Sedimentology and geochemistry of carbonates from lacustrine sequences in the Madrid Basin, central Spain. Chem Geol 123(1–4):173–191

Calvo JP, Alonso Zarza AM, Garcia del Cura MA, Ordonez S, Rodriguez-Aranda JP, Sanz Montero ME (1996) Sedimentary evolution of lake systems through the Miocene of the Madrid Basin: paleoclimatic and paleohydrological constraints. In: Friend PF, Dabrio CJ (eds) Tertiary basins of Spain: the stratigraphic record of crustal kinematics. University Press, Cambridge, pp 272–277

De Vicente G, Calvo JP, Munoz-Martin A (1996a) Neogene tectonosedimentary review of the Madrid Basin. In: Friend PF, Dabrio CJ (eds) Tertiary basins of Spain: the stratigraphic record of crustal kinematics. University Press, Cambridge, pp 268–271

De Vicente G, Gonzalez-Casado JM, Munoz-Martin A, Giner J, Rodriguez-Pascua MA (1996b) Structure and tertiary evolution of the Madrid Basin. In: Friend PF, Dabrio CJ (eds) Tertiary basins of Spain: the stratigraphic record of crustal kinematics. University Press, Cambridge, pp 263–267

Dean WE, Fouch TD (1983) Lacustrine environment. In: Scholle PA, Bebout DG, Moore CH (eds) Carbonate depositional environments. AAPG, Tulsa, pp 98–130

Dickson JAD (2002) Fossil echinoderms as monitor of the Mg/Ca ratio of the Phanerozoic oceans. Science 298:1222–1224

Dickson JAD (2004) Echinoderm skeletal preservation: calcite-aragonite Seas and the Mg/Ca ratio of Phanerozoic oceans. J Sediment Res 74(3):355–365

Ehrenberg SN (2004) Factors controlling porosity in Upper Carboniferous-Lower Permian carbonate strata of the Barents Sea. AAPG Bull 88(12):1653–1676

Ehrenberg SN, Boassen T (1993) Factors controlling permeability variation in sandstones of the Garn Formation in Trestakk Field, Norwegian continental shelf. J Sediment Res 63(5):929–944

Eugster HP, Kelts K (1983) Lacustrine chemical sediments. In: Goudie AS, Pye K (eds) Chemical sediments and geomorphology: precipitates and residua in the near-surface environment. Academic Press, London, pp 321–368

Hardie LA (1996) Secular variation in seawater chemistry: an explanation for the coupled secular variation in the mineralogies of marine limestones and potash evaporites over the past 600 m.y. Geology 24(3):279–283

Instituto geologico y minero de Espana (1975) Mapa geologico de Espana 1:50'000: Chinchon. Inst Tecnol Geomin Esp, Madrid

Junco F, Calvo JP (1983) Cuenca de Madrid. In: Geologia de Espana vol 2. Inst Tecnol Geomin Esp, Madrid, pp 534–543

Kelts K, Hsü KJ (1978) Freshwater carbonate sedimentation. In: Lerman A (ed) Lakes: chemistry, geology, physics. Springer, Berlin Heidelberg New York, pp 295–323

Lambert L, Durlet C, Loreau J-P, Marnier G (2006) Burial dissolution of micrite in Middle East carbonate reservoirs (Jurassic–Cretaceous): keys for recognition and timing. Mar Petrol Geol 23(1):79–92

Lasemi Z, Sandberg PA (1984) Transformation of aragonite-dominated lime muds to microcrystalline limestones. Geology 12(7):420–423

Lasemi Z, Sandberg PA (1993) Microfabric and compositional clues to dominant mud mineralogy of micrite precursors. In: Rezak R, Lavoie DL (eds) Carbonate microfabrics. Springer, Berlin Heidelberg New York, pp 173–185

Leng MJ, Lamb AL, Heaton THE, Marshall JD, Wolfe BB, Jones MD, Holmes JA, Arrowsmith C (2006) Isotopes in lake sediments. In: Leng MJ (ed) Isotopes in palaeoenvironmental research. Springer, Berlin Heidelberg New York, pp 147–184

Lerman A (1978) Lakes: chemistry, geology, physics. Springer, Berlin Heidelberg New York, p 363

Loreau J-P (1972) Pétrographie de calcaires fins au microscope électronique à balayage: introduction à une classification des micrites. C R Acad Sci Paris 274(6):810–813

Lowenstein TK, Timofeeff MN, Brennan ST, Hardie LA, Demicco RV (2001) Oscillations in Phanerozoic seawater chemistry: evidence from fluid inclusions. Science 294:1086–1088

Morse JW, Casey WH (1988) Ostwald processes and mineral paragenesis in sediments. Am J Sci 288(6):537–560

Moshier SO (1989) Microporosity in micritic limestones: a review. Sediment Geol 63(3–4):191–213

Munnecke A, Samtleben C (1996) The formation of micritic limestones and the development of limestone-marl alternations in the Silurian of Gotland, Sweden. Facies 34(1):159–176

Ostwald W (1887) Lehrbuch der Allgemeinen Chemie. Verlag von Wilhelm Engelmann, Leipzig, p 909

Perkins RD (1989) Origin of micro-rhombic calcite matrix within cretaceous reservoir rock, West Stuart City Trend, Texas. Sediment Geol 63(3–4):313–321

Richard J, Sizun JP, Machhour L (2007) Development and compartmentalization of chalky carbonate reservoirs: the Urgonian Jura-Bas Dauphine platform model (Genissiat, southeastern France). Sediment Geol 198(3–4):195–207

Sandberg PA (1983) An oscillating trend in phanerozoic non-skeletal carbonate mineralogy. Nature 305:19–22

Sanz ME (1994) Sedimentologia de las formaciones neogenas del sur de la Cuenca de Madrid, con enfasis en los procesos karsticos asociados a las rupturas sedimentarias del Plioceno. Dissertation, Universidad Complutense de Madrid

Sanz E, Sesé C, Calvo JP (1992) Primer hallazgo de Micromamiferos de edad turoliense en la Cuenca de Madrid. Estud Geol 48:171–178

Siemann MG (2003) Extensive and rapid changes in seawater chemistry during the Phanerozoic: evidence from Br contents in basal halite. Terra Nova 15(4):243–248

Stanley SM, Hardie LA (1998) Secular oscillations in the carbonate mineralogy of reef-building and sediment-producing organisms driven by tectonically forced shifts in seawater chemistry. Palaeogeogr Palaeoclimatol Palaeoecol 144(1–2):3–19

Teranes JL, McKenzie JA, Lotter AF, Sturm M (1999) Stable isotope response to lake eutrophication: calibration of a high-resolution lacustrine sequence from Baldeggersee, Switzerland. Limnol Oceanogr 44(2):320–333

Utrilla R, Vázquez A, Anadón P (1998) Paleohydrology of the Upper Miocene Bicorb Lake (eastern Spain) as inferred from stable isotopic data from inorganic carbonates. Sediment Geol 121(3–4): 191–206

Volery C, Davaud E, Foubert A, Caline B (2009) Shallow-marine microporous carbonate reservoir rocks in the Middle East: relationship with seawater Mg/Ca ratio and eustatic sea level. J Petrol Geol 32(4):313–325

Westphal H (2006) Limestone–marl alternations as environmental archives and the role of early diagenesis: a critical review. Int J Earth Sci 95(6):947–961

Wright VP, Alonzo Zarza AM, Sanz ME, Calvo JP (1997) Diagenesis of Late Miocene micritic lacustrine carbonates, Madrid Basin, Spain. Sediment Geol 114(1–4):81–95